

REPORT DOCUMENTATION PAGE				Form Approved OMB No. 0704-0188	
Public reporting burden for this collection of information is estimated to average 1 hour per response, including the time for reviewing instructions, searching existing data sources, gathering and maintaining the data needed, and completing and reviewing this collection of information. Send comments regarding this burden estimate or any other aspect of this collection of information, including suggestions for reducing this burden to Department of Defense, Washington Headquarters Services, Directorate for Information Operations and Reports (0704-0188), 1215 Jefferson Davis Highway, Suite 1204, Arlington, VA 22202-4302. Respondents should be aware that notwithstanding any other provision of law, no person shall be subject to any penalty for failing to comply with a collection of information if it does not display a currently valid OMB control number. <b>PLEASE DO NOT RETURN YOUR FORM TO THE ABOVE ADDRESS.</b>					
1. REPORT DATE (DD-MM-YYYY) 01-10-2003		2. REPORT TYPE Technical Paper		3. DATES COVERED (From - To)	
4. TITLE AND SUBTITLE  First Structural Characterization of Binary As(III) and Sb(III) Azides				5a. CONTRACT NUMBER F04611-99-C-0025	
				5b. GRANT NUMBER	
				5c. PROGRAM ELEMENT NUMBER	
6. AUTHOR(S)  Ralf Haiges (USC); Ashwani Vij and Jerry Boatz (AFRL/PRSP); Stefan Schneider, Thorsten Schroer, and Michael Gerken (USC); Karl Christe (ERC)				5d. PROJECT NUMBER DARP	
				5e. TASK NUMBER A205	
				5f. WORK UNIT NUMBER	
7. PERFORMING ORGANIZATION NAME(S) AND ADDRESS(ES)  ERC, Inc. 10 East Saturn Blvd. Edwards AFB CA 93524-7680				8. PERFORMING ORGANIZATION REPORT NUMBER	
9. SPONSORING / MONITORING AGENCY NAME(S) AND ADDRESS(ES)  Air Force Research Laboratory (AFMC) AFRL/PRS 5 Pollux Drive Edwards AFB CA 93524-7048				10. SPONSOR/MONITOR'S ACRONYM(S)	
				11. SPONSOR/MONITOR'S NUMBER(S) AFRL-PR-ED-TP-2003-247	
12. DISTRIBUTION / AVAILABILITY STATEMENT  Approved for public release; distribution unlimited.					
13. SUPPLEMENTARY NOTES For presentation in Chemistry – A European Journal.					
14. ABSTRACT  <div style="text-align: right; border: 1px solid black; padding: 10px; width: fit-content; margin: 20px auto;">20031017 124</div>					
15. SUBJECT TERMS					
16. SECURITY CLASSIFICATION OF:			17. LIMITATION OF ABSTRACT	18. NUMBER OF PAGES	19a. NAME OF RESPONSIBLE PERSON
a. REPORT Unclassified	b. ABSTRACT Unclassified	c. THIS PAGE Unclassified	A	38	Leilani Richardson
				19b. TELEPHONE NUMBER (include area code) (661) 275-5015	

# First Structural Characterization of Binary As(III) and Sb(III) Azides

Ralf Haiges,<sup>[a]</sup> Ashwani Vij,<sup>[b]</sup> Jerry A. Boatz,<sup>[b]</sup> Stefan Schneider,<sup>[a]</sup>

Thorsten Schroer,<sup>[a]</sup> Michael Gerken,<sup>[a]</sup> and Karl O. Christe<sup>\*,[a,b]</sup>

**Abstract:** The highly explosive molecules  $\text{As}(\text{N}_3)_3$  and  $\text{Sb}(\text{N}_3)_3$  were obtained for the first time in pure form by the reactions of the corresponding fluorides with  $(\text{CH}_3)_3\text{SiN}_3$  in  $\text{SO}_2$  solution and purification by sublimation. The crystal structures,  $^{14}\text{N}$  NMR and infrared and Raman spectra were determined and the results compared to ab initio second order perturbation theory calculations. Whereas  $\text{Sb}(\text{N}_3)_3$  possesses a propeller-shaped, pyramidal structure with perfect  $\text{C}_3$  symmetry, the  $\text{As}(\text{N}_3)_3$  molecule is significantly distorted from  $\text{C}_3$  symmetry due to crystal packing effects.

**Keywords:** antimony triazide · arsenic triazide · crystal structures · NMR spectroscopy · theoretical calculations · vibrational spectroscopy

---

[a] Dr. R. Haiges, Dr. S. Schneider, Dr. T. Schroer, Dr. M. Gerken, Prof. K. O. Christe  
Loker Research Institute  
University of Southern California  
Los Angeles, CA 90089-1661 (USA)  
Fax: (+1) 213-740-6679  
E-mail: kchriste@usc.edu  
and

[b] Dr. A. Vij, Dr. J. Boatz, Prof. K. O. Christe  
ERC, Inc. and Space and Missile Propulsion Division,  
Air Force Research Laboratory (AFRL/PRSP)  
10 East Saturn Boulevard, Bldg 8451  
Edwards Air Force Base, CA 93524 (USA)

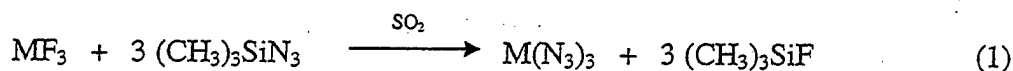
**DISTRIBUTION STATEMENT A**  
Approved for Public Release  
Distribution Unlimited

## Introduction

The syntheses of the highly explosive binary triazides of arsenic and antimony have recently been reported.<sup>[1-4]</sup> However, the structures of these interesting compounds could not be determined because they were difficult to crystallize or obtained only as oils. We have now been able to prepare  $M(N_3)_3$  ( $M=As, Sb$ ) as very pure solids and obtained their single crystals by slow and careful sublimation of the solids.

## Results and Discussion

**Syntheses and Properties:** The reaction of  $AsF_3$  or  $SbF_3$  in  $SO_2$  with excess  $(CH_3)_3SiN_3$  at room temperature results in complete azide-fluoride exchange yielding a clear solution of  $As(N_3)_3$  or precipitation of  $Sb(N_3)_3$ , respectively, according to eq. (1).



$M = As, Sb$

Removal of the volatile compounds,  $SO_2$ ,  $(CH_3)_3SiF$ , and excess  $(CH_3)_3SiN_3$ , at ambient temperature results in pure triazides.

$As(N_3)_3$ , which had previously been prepared by the reaction of  $AsCl_3$  with  $NaN_3$  and been reported to be a yellowish liquid,<sup>[1]</sup> was obtained as a white solid. Single crystals of arsenic triazide were obtained by slow and careful sublimation in a dynamic vacuum. The crystalline product melts at 37 °C. The molten  $As(N_3)_3$  decomposes at 62 °C, resulting in a milky liquid that explodes at about 160 °C.

Crude  $Sb(N_3)_3$  was isolated as a white solid with a decomposition point of 130 °C. Despite previous reports of explosive decomposition upon attempted sublimation,<sup>[2]</sup> we

were able to obtain colorless crystals by sublimation of the crude product in a static vacuum at 100-110 °C. It should be emphasized that  $\text{As}(\text{N}_3)_3$  and  $\text{Sb}(\text{N}_3)_3$  are sensitive to mechanical shock and can explode violently.

**Crystal structure of  $\text{As}(\text{N}_3)_3$ :** Clear colorless  $\text{As}(\text{N}_3)_3$  crystallizes in the monoclinic system (Table 1). The crystal structure of  $\text{As}(\text{N}_3)_3$  is shown in Fig. 1; and the atomic coordinates and bond distances are listed in Tables 2 and 3. The three azido groups are arranged in a pyramidal, propeller-type fashion, which is in contrast to the  $[\text{C}(\text{N}_3)_3]^+$  cation that exhibits a trigonal planar arrangement for the central carbon atom and the three *alpha*-nitrogen atoms.<sup>[5]</sup> This difference in the structures of  $\text{M}(\text{N}_3)_3$  ( $\text{M} = \text{As}, \text{Sb}$ ) and  $[\text{C}(\text{N}_3)_3]^+$  is due to the presence of a sterically active lone valence electron pair on As and Sb (see Figure 2).

In  $\text{As}(\text{N}_3)_3$ , the three azido groups point away from the arsenic lone pair. The torsion angles (Table 3) clearly show that the  $\text{As}(\text{N}_3)_3$  structure lacks perfect  $\text{C}_3$  symmetry. The values for the N7-As1-N4-N5 and N1-As1-N7-N8 angles are similar with 5.0(2) and 5.1(2)°, respectively, but different from the N4-As1-N1-N2 angle of 11.9(2)° indicating the presence of nonequivalent azido groups. A mean least squares planes analysis of the azido groups relative to the plane formed by the three *alpha*-nitrogen atoms further substantiates the nonequivalence of these groups. The relative twists of the azido groups N1-N2-N3, N4-N5-N6 and N7-N8-N9 compared to the mean plane formed by N1, N4 and N7 are 46.9(2), 43.0(2) and 57.9(3)°, respectively.

The packing diagram for  $\text{As}(\text{N}_3)_3$  is shown in Figures 3 and 4. It is well known that arsenic atoms can accommodate at least 6 closely packed fluoride ligands, as in  $\text{AsF}_6^-$ . It is, therefore, not surprising that arsenic seeks a coordination number higher than

4 in  $\text{As}(\text{N}_3)_3$ . For  $\text{SbCl}(\text{N}_3)_2$ , it has previously been shown<sup>[6]</sup> that the antimony atom can expand its coordination number by the formation of nitrogen bridges involving the  $\alpha$ -nitrogen atoms of the azido ligands. This bridging mode results in four-membered rings containing two antimony and two  $\text{N}_\alpha$  atoms. These rings are interconnected through the antimony atoms, thus forming infinite zigzag chains. The same bridging principle is observed for  $\text{As}(\text{N}_3)_3$  where two of its azido groups,  $\text{N1-N2-N3}$  and  $\text{N4-N5-N6}$ , participate in the formation of the infinite chain structure *via* formation of fused  $\text{As}_2\text{N1}_2$  and  $\text{As}_2\text{N4}_2$  dimeric parallelograms (see Figure 3). These chains run along the  $a$ -axis with the two parallelograms twisted at  $\sim 74^\circ$  with respect to each other. The bridge bond distances are 2.970 Å for the rings involving the N4 atoms and 3.069 Å for the rings involving the N1 atoms. The nonequivalence of the two rings is caused by N6 forming an additional bridge of 3.198 Å to an arsenic atom of a neighboring chain, perpendicular to  $ab$ -plane, thus interconnecting the individual chains to form a three dimensional network (see Figure 4). Like the chlorine ligand in  $\text{SbCl}(\text{N}_3)_2$ , the third azido ligand,  $\text{N7-N8-N9}$ , does not participate in the bridging. This packing arrangement accounts for the nonequivalence of the three azido ligands in  $\text{As}(\text{N}_3)_3$  and provides the arsenic atoms with a coordination number of 7 with 3 azido ligands, 3 nitrogen bridges, and one free valence electron pair. The arrangement is that of a distorted mono-capped octahedron, with the free valence electron pair occupying the mono-cap position. The angle, formed by the bridge bonds, is significantly larger than that between the azido ligands (Figure 2). The relative ease, with which crystal packing effects can deform the  $\text{As}(\text{N}_3)_3$  structure from the ideal  $\text{C}_3$  symmetry, is also supported by the theoretical calculations (see below). It

was found that the four stable isomers, which exhibit different orientations of the azido groups, differ in energy by a mere 3 kcal/mol or less.

**Crystal structure of  $\text{Sb}(\text{N}_3)_3$ :** This molecule ( Figure 5 and Tables 3 and 4) represents a "text-book" example of perfect  $C_3$  symmetry. The asymmetric  $\text{SbN}_3$  unit shows an azido group covalently bonded to the antimony atom which lies on a three fold rotational axis. The symmetry operations  $z, x, y$  and  $y, z, x$  for a rhombohedral setting for space group  $R-3$  generate the remaining two azido groups, thus placing the antimony atom at the pivot of a propeller shaped molecule. The Sb-N distance of 2.119(4) Å is shorter than the two Sb-N distances of 2.152(8) and 2.1444(7) Å found in the crystal structure of  $\text{SbCl}(\text{N}_3)_2$ .<sup>[6]</sup> The azido groups are almost linear with N-N-N angles of 178.3(5)°. As found for the  $\text{As}(\text{N}_3)_3$  structure, the  $\text{N}_\alpha\text{-N}_\beta$  distance of 1.233(6) Å is longer than the  $\text{N}_\beta\text{-N}_\gamma$  distance of 1.131(6) Å. However, in the case of  $\text{SbCl}(\text{N}_3)_2$ ,<sup>[6]</sup> one of the azido groups shows an "abnormal"  $\text{N}_\alpha\text{-N}_\beta$  distance of 0.98(1) Å which is shorter than the  $\text{N}_\beta\text{-N}_\gamma$  distance of 1.28(1) Å. This peculiarity has also been observed by us for a mixed chloride/azide antimony(V) anions,  $[\text{Ph}_4\text{M}]^+[\text{SbCl}_x(\text{N}_3)_{6-x}]^-$  ( $x = 2-5$ ;  $\text{M} = \text{P}$  or  $\text{As}$ )<sup>[7]</sup> and by others for the structures of some azido derivatives of platinum,<sup>[8-10]</sup> vanadium,<sup>[11]</sup> and tantalum.<sup>[12]</sup> In our opinion, these unusually short distances are not real and are due to partial occupancy of some azide sites by other atoms, such as chlorine.

In  $\text{Sb}(\text{N}_3)_3$  and  $\text{SbCl}(\text{N}_3)_2$ , the angles at the Sb atom are compressed from an ideal tetrahedral value of 109.5° to ~90°. This angle compression is caused by the increased repulsion from the sterically active free valence electron pair on antimony. Because this effect increases with increasing size of the central atom, it is less pronounced for  $\text{As}(\text{N}_3)_3$ , which exhibits an N-As-N angle of 97.9°. Furthermore, the Sb-N-N angles of 115.8(3)° in

$\text{Sb}(\text{N}_3)_3$  are smaller than those of  $\sim 120^\circ$  found in  $\text{SbCl}(\text{N}_3)_2$ .<sup>[6]</sup> In accord with the requirements for  $C_3$  symmetry, the torsion angles in  $\text{Sb}(\text{N}_3)_3$  are all identical and, due to the almost linear azide group ( $178.3(5)^\circ$ ), the M-N-N-N torsion angles are poorly determined.

One of the most interesting consequences of the high symmetry of  $\text{Sb}(\text{N}_3)_3$  is its crystal packing. Figure 6 shows aesthetically pleasing views down the  $z$  (1 1 1) axis. Each of the molecules has a three-fold local symmetry, but the  $z$ -axis also constitutes the crystallographic three-fold axis. When no bonds are displayed, the nitrogen packing mimics the "Star of David". However, when all bonds are displayed, an inorganic pseudo-18-crown-6 evolves in which six antimony atoms form a perfect hexagon and encapsulate two  $\text{Sb}(\text{N}_3)_3$  molecules located on a pseudo- $S_6$  axis passing through the center of the hexagonal cell. The two central  $\text{Sb}(\text{N}_3)_3$  molecules are stacked with the lone-pairs on antimony pointing away from each other and the three azido groups on each antimony being rotated by  $60^\circ$  from each other, forming a perfectly staggered structure. When viewed from the top, each individual  $\text{Sb}(\text{N}_3)_3$  unit resembles the three legged "Isle of Man" emblem.

When viewed from the side (see Figure 7), the packing can be described as a sheet structure. Within each sheet, there are two  $\text{Sb}(\text{N}_3)_3$  layers. The antimony atoms of each layer point in opposite directions and form triangular funnel-like holes. The antimony atoms of one layer are located deep inside the holes of the other layer and reside  $\sim 0.9 \text{ \AA}$  beyond the plane formed by the antimony atoms of the other layer. The resulting close contact between the two layers allows each antimony to form three close contacts of  $2.844 \text{ \AA}$  with  $\alpha$ -nitrogen atoms from three neighboring  $\text{Sb}(\text{N}_3)_3$  units, thus creating two-

dimensional sheets (see Figure 8). This gives antimony a total coordination number of seven (three equivalent azido ligands, three equivalent nitrogen bridges, and one sterically active free valence electron pair). Because of the increased repulsion from the free valence electron pair of antimony, the angle between the Sb...N bridges is opened to  $118.7^\circ$  while the N-Sb-N angle is compressed to about  $90^\circ$ . The Sb...N bridges result in the formation of three  $\alpha$ -nitrogen-bridged, perfectly planar, four-membered rings around each antimony atom. A mean least square plane analysis shows that they form angles of  $76.6^\circ$  with each other and are arranged in a fashion resembling the "Mitsubishi" emblem (see insert in Figure 8). The contacts between the sheets consist of staggered azido groups that are rotated by  $60^\circ$  with respect to each other.

The  $\text{Sb}(\text{N}_3)_3$  and  $\text{As}(\text{N}_3)_3$  packings have several features in common. In both structures, the central atoms have coordination numbers of seven with three azide ligands, three nitrogen bridges, and one sterically active free valence electron pair. Furthermore, both molecules associate through the formation of  $\text{N}_\alpha$ -bridged four-membered rings. However, in  $\text{Sb}(\text{N}_3)_3$ , all three  $\text{N}_\alpha$ -atoms participate equally in the bridge formation (see "Mitsubishi" insert in Figure 8), while in  $\text{As}(\text{N}_3)_3$  only two  $\text{N}_\alpha$ -atoms and one  $\text{N}_\gamma$ -atom are involved ("Half-Mitsubishi", see Figure 9). This results in a ribbon-like structure for  $\text{As}(\text{N}_3)_3$  and a sheet structure for  $\text{Sb}(\text{N}_3)_3$ . Also, the bridges in  $\text{Sb}(\text{N}_3)_3$  are much stronger ( $2.844 \text{ \AA}$ , while the sum of the covalent Van der Waals radii is  $3.66 \text{ \AA}$ ) than those in  $\text{As}(\text{N}_3)_3$  ( $2.970$ ,  $3.069$ , and  $3.198 \text{ \AA}$ , while the sum of the covalent Van der Waals radii is only  $3.40 \text{ \AA}$ ).

**$^{14}\text{N}$  NMR Spectra:** As expected for covalently bonded azides,<sup>[4]</sup> three well resolved resonances were found for both compounds in their  $^{14}\text{N}$  NMR spectra in  $\text{CH}_2\text{Cl}_2$  solution



at 25 °C. The  $\text{As}(\text{N}_3)_3$  molecule shows a very broad signal at  $\delta = -290$  ppm ( $\Delta\nu_{1/2} = 300$  Hz) for the  $\text{N}_\alpha$  atoms, a sharp signal at  $\delta = -145.3$  ppm ( $\Delta\nu_{1/2} = 14$  Hz) for the  $\text{N}_\beta$  atoms, and a medium-sharp resonance at  $\delta = -175.9$  ppm ( $\Delta\nu_{1/2} = 34$  Hz) for the  $\text{N}_\gamma$  atoms. This is in disagreement with the data previously reported for this compound,  $\delta = -318.0$  ppm ( $\text{N}_\alpha$ ),  $-131.1$  ppm ( $\text{N}_\beta$ ), and  $-165.2$  ppm ( $\text{N}_\gamma$ ).<sup>[1,13]</sup> However, the observed  $^{14}\text{N}$  NMR resonances for  $\text{Sb}(\text{N}_3)_3$  of  $\delta = -324.5$  ppm ( $\Delta\nu_{1/2} = 139$  Hz,  $\text{N}_\alpha$ ),  $-136.2$  ppm ( $\Delta\nu_{1/2} = 18$  Hz,  $\text{N}_\beta$ ) and  $-172.3$  ppm ( $\Delta\nu_{1/2} = 23$  Hz,  $\text{N}_\gamma$ ) are in good agreement with the data, reported previously.<sup>[2]</sup>

**Theoretical Calculations:** Geometry optimizations were performed for  $\text{As}(\text{N}_3)_3$  and  $\text{Sb}(\text{N}_3)_3$  using second order perturbation theory methods (MP2, also known as MBPT(2)).<sup>[14,15]</sup> All stationary points were verified as local minima via diagonalization of the matrix of energy second derivatives with respect to nuclear displacements (i.e., the hessian matrix).

Four local minima were located for  $\text{As}(\text{N}_3)_3$  (see Figure 10). Zero-point vibrational energy corrections for these minima differed by less than 0.1 kcal/mol. In the most stable minimum at the MP2 level, (**3**,  $\text{C}_1$ ), two azido ligands adopt an approximate anti orientation relative to the stereochemically active lone pair on the As atom, with the remaining azido ligand in a gauche-like orientation. The second most stable isomer (**1**,  $\text{C}_3$ ) is 0.4 kcal/mol higher in energy than **3** and has all three azido ligands in an anti orientation. The isomer with two gauche azido ligands and one anti azido ligand (**2**) has  $\text{C}_s$  symmetry and is 0.7 kcal/mol higher in energy than **3**. Finally, the least stable minimum (**4**) has all three azido groups in a gauche orientation ( $\text{C}_3$  symmetry) and is 3.0 kcal/mol higher in energy than **3**. The observed crystal structure is best described as a

somewhat distorted  $C_3$  structure with the three azido ligands in an anti configuration. The calculated small energy differences can account for the ease with which this compound can distort from the ideal  $C_3$  symmetry under the influence of crystal packing effects.

For  $Sb(N_3)_3$ , two local minima with  $C_3$  and  $C_1$  symmetry were located, with virtually identical zero-point vibrational energy corrections. The  $C_3$  structure has all azido ligands oriented anti with respect to the Sb lone pair. In the  $C_1$  minimum, which is 0.6 kcal/mol less stable than the  $C_3$  isomer, two azido ligands are anti and the third azide is gauche (see Figure 10).

**Vibrational Spectra:** The infrared and Raman spectra of  $As(N_3)_3$  and  $Sb(N_3)_3$  are shown in Figures 11 and 12, respectively. Tables 5 and 6 summarize the computed and observed frequencies. The vibrational spectra of both compounds demonstrate the presence of covalently bonded azido ligands. The presence of more than one azido ligand results in in-phase and out-of-phase coupling, and the internal azido modes split into two components. For  $C_3$  symmetry, the out-of-phase E modes are doubly degenerate and, in some cases, can be split due to a lifting of the degeneracy. The observation of extra bands in the 1350 to 1100  $cm^{-1}$  region is attributed to Fermi resonance of  $\nu_2$  and  $\nu_{10}$  with the appropriate combination bands or overtones.

For  $As(N_3)_3$ , the best fit between observed and computed frequencies is obtained for the  $C_3(\underline{1})$  isomer, in accord with the observed crystal structure. The fit between observed and calculated frequencies is good for both  $As(N_3)_3$  and  $Sb(N_3)_3$ . As might be expected, the nitrogen bridging lowers the skeletal  $AsN_3$  and  $SbN_3$  stretching frequencies and increases those of the deformation modes. This effect is more pronounced for  $Sb(N_3)_3$  because of the stronger bridging. The general agreement between the vibrational

spectra of  $\text{As}(\text{N}_3)_3$  and  $\text{Sb}(\text{N}_3)_3$  is very good and supports our vibrational analysis. The only ambiguity is the observation of one weak Raman at 191 and 211  $\text{cm}^{-1}$  in  $\text{As}(\text{N}_3)_3$  and  $\text{Sb}(\text{N}_3)_3$ , respectively, which could not be accounted for in our assignments and were tentatively assigned to a stretching mode involving the nitrogen bridges.

### Conclusion

The exact structures of the highly explosive  $\text{As}(\text{N}_3)_3$  and  $\text{Sb}(\text{N}_3)_3$  molecules have been determined for the first time. Both structures can be derived from an ideal  $\text{C}_3$  symmetry with the azido ligands being bent away from the sterically active free valence electron pair of the central atom. Additional nitrogen bridging increases the coordination numbers of arsenic and antimony to 7. The basic motif for the nitrogen bridging are four-membered, dimeric rings consisting of two As or Sb atoms and two alpha-nitrogen atoms from two azido ligands. For  $\text{As}(\text{N}_3)_3$ , only two of its three azido ligands participate in the association process, resulting in an infinite zigzag chain structure and destroying the perfect  $\text{C}_3$  symmetry. For  $\text{Sb}(\text{N}_3)_3$ , however, all three azido ligands take part equally in the association and produce a highly symmetrical sheet structure, representing a case of perfect rhombohedral  $\text{C}_3$  symmetry.

### Experimental Section

*Caution! Arsenic and antimony azide compounds are potentially toxic and can decompose explosively under various conditions! They should be handled only on a small*

*scale with appropriate safety precautions (face shields, leather gloves and protective clothing).*

**Materials and Apparatus.** All reactions were carried out in Teflon-FEP ampules that were closed by stainless steel valves. Volatile materials were handled in a stainless steel-Teflon-FEP or Pyrex glass vacuum line. All reaction vessels and the stainless steel line were passivated with  $\text{ClF}_3$  prior to use. Nonvolatile materials were handled in the dry argon atmosphere of a glove box.

Infrared spectra were recorded in the range  $4000\text{--}400\text{ cm}^{-1}$  on a Midac FT-IR model 1720 at a resolution of  $1\text{ cm}^{-1}$ . Spectra of solids were obtained by using dry powders pressed between AgCl windows in an Econo press (Barnes Engineering Co.). Raman spectra were recorded in the range  $4000\text{--}80\text{ cm}^{-1}$  on a Bruker Equinox 55 FT-RA spectrophotometer using a Nd:YAG laser at 1064 nm. Pyrex melting point tubes that were baked out at  $300\text{ }^\circ\text{C}$  for 48 h at 10 mTorr vacuum or Teflon-FEP tubes with stainless steel valves that were passivated with  $\text{ClF}_3$  were used as sample containers.

$^{14}\text{N}$  NMR spectra were recorded at 36.13 MHz on a Bruker AMX 500 spectrometer using  $\text{CH}_2\text{Cl}_2$  solutions in sealed standard glass tubes. Neat  $\text{CH}_3\text{NO}$  ( $\delta = 0.00\text{ ppm}$ ) was used as external reference for  $^{14}\text{N}$ .

The  $(\text{CH}_3)_3\text{SiN}_3$  (Aldrich) and  $\text{AsF}_3$  (Ozark) were purified by fractional condensation prior to use. The  $\text{SbF}_3$  (Alfa Aesar) was purified by sublimation. The  $\text{SO}_2$  (Aldrich) was condensed into a bulb and dried over  $\text{CaH}_2$ .

**Preparation of  $\text{As}(\text{N}_3)_3$ .** On the stainless steel vacuum line,  $\text{AsF}_3$  (0.23 mmol) was condensed at  $-196\text{ }^\circ\text{C}$  into a Teflon-FEP ampule. The ampule was then attached to a glass vacuum line and after evacuation,  $\text{SO}_2$  (3.3 mmol) was condensed in at  $-196\text{ }^\circ\text{C}$ . The

mixture was allowed to warm to ambient temperature. After all the  $\text{AsF}_3$  had dissolved, the ampule was cooled back again to  $-196^\circ\text{C}$ , and  $(\text{CH}_3)_3\text{SiN}_3$  (0.885 mmol) was added. The ampule was kept at  $-40^\circ\text{C}$  for 30 min and then slowly warmed to room temperature over a period of 4 h, resulting in a colorless solution. The volatile components were pumped off, leaving behind a white solid (0.045 g, weight calculated for 0.23 mmol  $\text{As}(\text{N}_3)_3 = 0.046$  g). Further pumping at ambient temperature led to the sublimation of the crude product resulting in the formation of crystalline material on the walls of the reaction vessel. Inspection of the volatile material trapped at  $-196^\circ\text{C}$  by gas-FTIR spectroscopy showed  $\text{SO}_2$  and  $(\text{CH}_3)_3\text{SiF}^{[16,17]}$  as the only reaction by-products. The crystalline solid was identified as  $\text{As}(\text{N}_3)_3$  by vibrational and NMR spectroscopy and its crystal structure.

**Preparation of  $\text{Sb}(\text{N}_3)_3$ .** A sample of  $\text{SbF}_3$  (0.47 mmol) was loaded in the dry box into a Teflon-FEP ampule, followed by the addition of  $\text{SO}_2$  (5.8 mmol) *in vacuo* at  $-196^\circ\text{C}$ . The mixture was warmed to room temperature to suspend the  $\text{SbF}_3$  in the  $\text{SO}_2$ , cooled back again to  $-196^\circ\text{C}$ , and  $(\text{CH}_3)_3\text{SiN}_3$  (2.16 mmol) was condensed in. The ampule was kept at  $-40^\circ\text{C}$  for 30 min and then slowly warmed to ambient temperature over a period of 4 h. Volatile components were pumped off and collected at  $-196^\circ\text{C}$ , leaving behind a white solid residue (0.120 g, weight calculated for 0.47 mmol of  $\text{Sb}(\text{N}_3)_3 = 0.116$  g). The only volatile by-product, identified by gas-FTIR spectroscopy, was  $(\text{CH}_3)_3\text{SiF}$ . The crude  $\text{Sb}(\text{N}_3)_3$  was vacuum sublimed in a sealed glass tube at  $100$ - $110^\circ\text{C}$ . The obtained colorless crystals were characterized by vibrational and NMR spectroscopy and their crystal structure.

**Crystal Structure Determinations.** The single crystal x-ray diffraction data were

collected on a Bruker 3-circle platform diffractometer, equipped with a SMART CCD (charge coupled device) detector, with the  $\chi$ -axis fixed at  $54.74^\circ$  and using  $\text{MoK}_\alpha$  radiation ( $\lambda = 0.71073 \text{ \AA}$ ) from a fine-focus tube. An LT-3 apparatus was employed for the low-temperature data collection using controlled liquid nitrogen boil off. A few well-formed single crystals, prepared by careful sublimation of the amorphous solid, were selected in a glove box, using a CCD camera microscope. The selected crystals were immersed in PFPE (perfluoropolyether) oil, contained in the cavity of a culture slide. A Cryoloop was used for picking a crystal and mounting it on a magnetic goniometer head. Cell constants were determined from 90 ten-second frames. A complete hemisphere of data was scanned on omega ( $0.3^\circ$ ) with a run time of thirty-seconds per frame at a detector resolution of  $512 \times 512$  pixels using the SMART software.<sup>[18]</sup> A total of 1271 frames was collected in three sets and a final set of 50 frames, identical to the first 50 frames, was also collected to determine any crystal decay. The frames were then processed on a PC running on Windows NT software. The SAINT software<sup>[19]</sup> was used to obtain the hkl file corrected for  $L_p$ /decay. The absorption correction was performed using the SADABS program.<sup>[20]</sup> For  $\text{As}(\text{N}_3)_3$ , the intensity statistics, i.e.,  $E^2-1$  values, indicated a centrosymmetric space group. Furthermore, the absence of  $0\ k\ 0$  ( $k = \text{odd}$ ) and  $h0l$  reflections ( $h+l = \text{odd}$ ) showed the presence of a  $2_1$  screw axis and a  $c$ -glide plane parallel and perpendicular to the  $b$ -axis, respectively. The space group was thus unambiguously assigned as  $P2_1/c$ . For  $\text{Sb}(\text{N}_3)_3$ , the reciprocal lattice was initially indexed as a hexagonal cell with cell constants of  $a = 7.2046(10) \text{ \AA}$ ,  $c = 19.439(4) \text{ \AA}$ ,  $V = 873.8(2) \text{ \AA}^3$  and  $Z = 6$ . An alternate setting with a smaller rhombohedral cell was obtained by using the transformation matrix  $\{\frac{2}{3}, \frac{1}{3}, \frac{1}{3}, -\frac{1}{3}, \frac{1}{3}, \frac{1}{3}, -\frac{1}{3}, -\frac{2}{3}, \frac{1}{3}\}$  with cell

constants of  $a = 7.6998(9)$ ,  $\alpha = 55.787(17)^\circ$ ,  $V = 291.26(6) \text{ \AA}^3$  and  $Z = 2$ . The structures were solved by the Patterson method using the SHELX-90 program<sup>[21]</sup> and refined by the least squares method on  $F^2$ , SHELXL-97,<sup>[22]</sup> incorporated in the SHELXTL Suite 5.10 for Windows NT.<sup>[23]</sup> All atoms were refined anisotropically. For the anisotropic displacement parameters, the  $U(\text{eq})$  is defined as one third of the trace of the orthogonalized  $U_{ij}$  tensor. CCDC-XXX and CCDC-XXX contain the supplementary crystallographic data for  $\text{As}(\text{N}_3)_3$  and  $\text{Sb}(\text{N}_3)_3$ , respectively. These data can be obtained free of charge via [www.ccdc.cam.ac.uk/conts/retrieving.html](http://www.ccdc.cam.ac.uk/conts/retrieving.html) (or from the Cambridge Crystallographic Data Centre, 12 Union Road, Cambridge CB21EZ, UK; fax: (+44) 1223-336-033; or [deposit@ccdc.cam.ac.uk](mailto:deposit@ccdc.cam.ac.uk)).

**Computational Methods.** Optimizations of all structures were performed using second order perturbation theory.<sup>[14,15]</sup> For  $\text{As}(\text{N}_3)_3$ , the Binning and Curtis double-zeta valence basis set,<sup>[24]</sup> augmented with a d polarization function<sup>[25]</sup> was used for arsenic and the 6-31G(d) basis set<sup>[26,27]</sup> for nitrogen. For  $\text{Sb}(\text{N}_3)_3$ , the Stevens, Basch, and Krauss effective core potentials and the corresponding valence-only basis sets were used.<sup>[28]</sup> The SBK valence basis set for nitrogen was augmented with a d polarization function<sup>[27]</sup> and a diffuse s+p shell,<sup>[29]</sup> whereas only a d polarization function<sup>[30]</sup> was added to the antimony basis set. Hessians (energy second derivatives) were calculated for the final equilibrium structures to determine if they are minima (positive definite hessian) or transition states (one negative eigenvalue). All calculations were performed using the electronic structure code GAMESS.<sup>[31]</sup>

### Acknowledgements

We are grateful to the National Science Foundation, the Air Force Office of Scientific Research and Defense Advance Research Projects Agency for financial support. One of us (R. H.) is grateful to the Deutsche Forschungsgemeinschaft for a stipend. A grant of computer time by the Department of Defense High Performance Computing Modernization Program at the Aeronautical Systems Center (Wright-Patterson AFB, OH) and Army High Performance Computing Research Center (Minneapolis, MN) is gratefully acknowledged.



## References

- [1] T. M. Klapötke, P. Geissler, *J. Chem. Soc. Dalton Trans.* **1995**, 3365.
- [2] T. M. Klapötke, A. Schulz, J. McNamara, *J. Chem. Soc. Dalton Trans.* **1996**, 2985.
- [3] K. Karaghiosoff, T. M. Klapötke, B. Krumm, H. Nöth, T. Schütt, M. Suter, *Inorg. Chem.* **2002**, *41*, 170.
- [4] For a recent review, see F. Fraenk, T. M. Klapötke, in *Inorganic Chemistry Highlights* (Eds.: G. Meyer, D. Naumann, L. Wesemann), Wiley-VCH, Weinheim, **2002**.
- [5] (a) U. Mueller, H. Baernighausen, *Acta Crystallogr.* **1970**, *B26*, 1671; (b) W. Kolitsch, U. Mueller, *Z. Anorg. Allg. Chem.* **1974**, *410*, 21; (c) M. A. Petrie, J. A. Sheehy, J. A. Boatz, G. Rasul, G. K. S. Prakash, G. A. Olah, K. O. Christe, *J. Am. Chem. Soc.* **1997**, *119*, 8802.
- [6] T. M. Klapötke, H. Nöth, T. Schütt, M. Warchold, *Z. Anorg. Allg. Chem.* **2001**, *627*, 81.
- [7] A. Vij, unpublished results.
- [8] B. Neumüller, F. Schmock, S. Schlecht, K. Dehnicke, *Z. Anorg. Allg. Chem.* **2000**, *626*, 1972.
- [9] M. Atam, U. Mueller, *J. Organomet. Chem.* **1974**, *71*, 435.
- [10] S. Schroeder, W. Preetz, *Z. Anorg. Allg. Chem.* **2001**, *627*, 390.
- [11] M. Herberhold, A.-M. Dietel, W. Milius, *Z. Anorg. Allg. Chem.* **1999**, *625*, 1885.
- [12] M. Herberhold, A. Goller, W. Milius, *Z. Anorg. Allg. Chem.* **2001**, *627*, 891.

- [13] P. Geissler, T. M. Klapötke, H.-J. Kroth, *J. Spectrochim. Acta* **1995**, *51A*, 1075.
- [14] (a) C. Moller, M. S. Plesset, *Phys. Rev.* **1934**, *46*, 618; (b) J.A. Pople, J.S. Binkley, R. Seeger, *Int. J. Quantum Chem. S10*, **1976**, 1; (c) M.J. Frisch, M. Head-Gordon, J.A. Pople, *Chem. Phys. Lett.* **1990**, *166*, 275.
- [15] R.J. Bartlett, D.M. Silver, *Int. J. Quantum Chem. Symp.* **1975**, *9*, 1927.
- [16] K. Licht, P. Koehler, H. Kriegsmann, *Z. Anorg. Allg. Chem.* **1975**, *415*, 31.
- [17] H. Bürger, *Spectrochim. Acta* **1968**, *24A*, 2015.
- [18] SMART V 4.045 Software for the CCD Detector System, Bruker AXS, Madison, WI (1999).
- [19] SAINT V 4.035 Software for the CCD Detector System, Bruker AXS, Madison, WI (1999).
- [20] SADABS Program for absorption correction for area detectors, Version 2.01, Bruker AXS, Madison, WI (2000).
- [21] G. M. Sheldrick, SHELXS-90, Program for the Solution of Crystal Structure, University of Göttingen, Germany, (1990).
- [22] G. M. Sheldrick, SHELXL-97, Program for the Refinement of Crystal Structure, University of Göttingen, Germany, (1997).
- [23] SHELXTL 5.10 for Windows NT, Program library for Structure Solution and Molecular Graphics, Bruker AXS, Madison, WI (1997).
- [24] R.C. Binning, Jr., L.A. Curtiss, *J. Comput. Chem.* **1990**, *11*, 1206.
- [25] A d-function polarization exponent of 0.293 was used.
- [26] W.J. Hehre, R. Ditchfield, J.A. Pople, *J. Chem. Phys.* **1972**, *56*, 2257.

- [27] The exponent of the d polarization function on N is 0.8; see P.C. Hariharan, J.A. Pople, *Theoret. Chim. Acta* **1973**, *28*, 213.
- [28] W.J. Stevens, H. Basch, M. Krauss, *J. Chem. Phys.* **1984**, *81*, 6026.
- [29] The exponent of the diffuse s+p shell is 0.0639; see T. Clark, J. Chandrasekhar, G.W. Spitznagel, P. von R. Schleyer, *J. Comput. Chem.* **1983**, *4*, 294.
- [30] The exponent of the d polarization function on Sb is 0.211; see S. Huzinaga, J. Andzelm, M. Klobukowski, E. Radzio-Andzelm, Y. Sakai, H. Tatewaki, "Gaussian Basis Sets for Molecular Calculations" Elsevier, Amsterdam, 1984.
- [31] M. W. Schmidt, K. K. Baldridge, J. A. Boatz, S. T. Elbert, M. S. Gordon, J. H. Jensen, S. Koseki, N. Matsunaga, K. A. Nguyen, S. Su, T. L. Windus, *J. Comput. Chem.* **1993**, *14*, 1347.

Table 1. Crystal data and structure refinement for As(N<sub>3</sub>)<sub>3</sub> and Sb(N<sub>3</sub>)<sub>3</sub>.

empirical formula	AsN <sub>9</sub>	N <sub>9</sub> Sb
fw	201.01	247.84
Temperature (K)	213(2)	223(2)
space group	<i>P</i> 2 <sub>1</sub> / <i>c</i>	<i>R</i> -3
<i>a</i> , Å	7.3263(7)	7.6998(9)
<i>b</i> , Å	11.7162(11)	
<i>c</i> , Å	6.9865(7)	
$\alpha$ , deg	90	55.787(17)
$\beta$ , deg	107.219(2)	
<i>V</i> , Å <sup>3</sup>	572.82(10)	291.26(6)
<i>Z</i>	4	2
$\rho_{\text{calc}}$ g/cm <sup>3</sup>	2.331	2.826
$\mu$ , mm <sup>-1</sup>	5.863	4.667
crystal size, mm	0.34 x 0.25 x 0.14	0.12 x 0.10 x 0.08
$\lambda$ , Å	0.71073	0.71073
<i>R</i> <sub>int</sub>	0.0272	0.0422
transmission factors	0.4941, 0.2404	0.7065, 0.6043
goodness-of-fit on <i>F</i>	1.098	1.132
<i>R</i> 1, <i>wR</i> 2 [ <i>I</i> > 2σ( <i>I</i> )]	0.0240 0.0641	0.0320, 0.0849
<i>R</i> 1, <i>wR</i> 2 (all data)	0.0254, 0.0650	0.0328, 0.0856

Table 2. Atomic coordinates ( $\times 10^4$ ) and equivalent isotropic displacement parameters ( $\text{\AA}^2 \times 10^3$ ) for  $\text{As}(\text{N}_3)_3$ .  $U(\text{eq})$  is defined as one third of the trace of the orthogonalized  $U_{ij}$  tensor.

	x	y	z	$U(\text{eq})$
As(1)	2858(1)	4451(1)	6183(1)	21(1)
N(1)	1116(3)	4819(2)	3655(3)	27(1)
N(2)	1725(3)	4783(2)	2190(3)	22(1)
N(3)	2190(3)	4790(2)	799(3)	35(1)
N(4)	4850(3)	3837(2)	5241(3)	25(1)
N(5)	4994(2)	2785(2)	5223(3)	23(1)
N(6)	5226(3)	1840(2)	5180(4)	37(1)
N(7)	1743(3)	3030(2)	6499(3)	26(1)
N(8)	250(3)	2776(2)	5209(3)	27(1)
N(9)	-1129(3)	2495(2)	4091(4)	41(1)

Table 3. Bond lengths [ $\text{\AA}$ ] and angles [ $^\circ$ ] for  $\text{As}(\text{N}_3)_3$  and  $\text{Sb}(\text{N}_3)_3$ .

	$\text{As}(\text{N}_3)_3$	$\text{Sb}(\text{N}_3)_3$
<i>Bond Distances (<math>\text{\AA}</math>)</i>		
M-N1	1.897(2)	2.119(4)
M-N4	1.910(2)	2.119(4) <sup>a</sup>
M-N7	1.896(2)	2.119(4) <sup>b</sup>
N(1)-N(2)	1.232(3)	1.233(6)
N(2)-N(3)	1.121(3)	1.131(6)
N(4)-N(5)	1.237(3)	1.233(6) <sup>a</sup>
N(5)-N(6)	1.122(3)	1.131(6) <sup>a</sup>
N(7)-N(8)	1.231(3)	1.233(6) <sup>b</sup>
N(8)-N(9)	1.128(3)	1.131(6) <sup>b</sup>
<i>Bond angles (<math>^\circ</math>)</i>		
N(1)-M-N(4)	97.87(9)	90.1(2)
N(1)-M-N(7)	96.51(9)	90.1(2) <sup>a</sup>
N(7)-M-N(4)	96.22(8)	90.1(2) <sup>b</sup>
N(2)-N(1)-M	117.1(2)	115.8(3)
N(5)-N(4)-M	117.1(2)	115.8(3) <sup>a</sup>
N(8)-N(7)-M	116.6(2)	115.8(3) <sup>b</sup>
N(3)-N(2)-N(1)	175.9(2)	178.3(5)
N(6)-N(5)-N(4)	175.8(2)	178.3(5) <sup>a</sup>
N(9)-N(8)-N(7)	176.3(2)	178.3(5) <sup>b</sup>
<i>Torsion angles (<math>^\circ</math>)</i>		
M-N(1)-N(2)-N(3)	161(4)	148(17)
M-N(4)-N(5)-N(6)	171(4)	
M-N(7)-N(8)-N(9)	171(4)	
N(1)-M-N(4)-N(5)	102.5(2)	
N(1)-M-N(7)-N(8)	5.1(2)	
N(4)-M-N(1)-N(2)	11.9(2)	9.9(3)
N(4)-M-N(7)-N(8)	103.8(2)	
N(7)-M-N(1)-N(2)	109.1(2)	100.1(3)
N(7)-M-N(4)-N(5)	5.0(2)	
$a = z, x, y$ ; $b = y, z, x$		

Table 4. Atomic coordinates ( $\times 10^4$ ) and equivalent isotropic displacement parameters ( $\text{\AA}^2 \times 10^3$ ) for  $\text{Sb}(\text{N}_3)_3$ .  $U(\text{eq})$  is defined as one third of the trace of the orthogonalized  $U_{ij}$  tensor.

	x	y	z	$U(\text{eq})$
Sb(1)	6897(1)	6897(1)	6897(1)	21(1)
N(1)	8642(6)	6330(6)	3834(7)	22(1)
N(2)	7558(7)	7362(7)	2605(7)	24(1)
N(3)	6612(8)	8311(8)	1432(8)	39(1)

Table 5. Comparison of observed and unscaled calculated MP2 vibrational frequencies ( $\text{cm}^{-1}$ ) and intensities for  $\text{C}_3(1)\text{As}(\text{N}_3)_3$ .

mode	approx. mode description		observed <sup>[a],[g]</sup>		calculated <sup>[b]</sup>
	in point group $\text{C}_3$		IR	Raman	(IR) [Raman]
A	$\nu_1$	$\nu_{\text{as}}\text{N}_3$ in phase	2121 (vs)	2128 [3.1]	2255 (506.9) [6.7]
	$\nu_2$	$\nu_s\text{N}_3$ in phase	1251 (s,sh) <sup>[e]</sup>	1257 [1.2] <sup>[e]</sup>	1293 (122.8) [22.1]
	$\nu_3$	$\delta\text{N}_3$ in phase, in plane		663 [1.7]	681 (0.7) [16.6]
	$\nu_4$	$\delta\text{N}_3$ in phase, out of plane			532 (0.2) [0.8]
	$\nu_5$	$\nu_s\text{AsN}_3$	480 (m)	465 [10.0]	507 (27.3) [23.4]
	$\nu_6$	$\delta\text{AsN}_3$ in phase	<sup>[c]</sup>	307 [0.3]	325 (35.5) [0.4]
	$\nu_7$	$\delta\text{As-N-N}$ in phase	<sup>[c]</sup>	102 [2.7]	94 (0.2) [1.0]
	$\nu_8$	$\tau$ in-phase	<sup>[c]</sup>	<sup>[d]</sup>	57.4 (0.0) [8.6]
E	$\nu_9$	$\nu_{\text{as}}\text{N}_3$ out of phase	2092 (vs)	2103 [2.1] <sup>[e]</sup> 2093 [1.8] <sup>[e]</sup>	2215 (298.3) [6.1]
	$\nu_{10}$	$\nu_s\text{N}_3$ out of phase	1231 (s)	1244 [0.3] <sup>[e,f]</sup> 1237 [0.2] <sup>[e,f]</sup>	1280 (92.8) [6.8]
	$\nu_{11}$	$\delta\text{N}_3$ out of phase, in plane	664 (m)		673 (25.3) [2.4]
	$\nu_{12}$	$\delta\text{N}_3$ out of phase, out of plane	568 (m)		532 (10.1) [0.7]
	$\nu_{13}$	$\nu_{\text{as}}\text{AsN}_3$	420 (s)	419 [4.6]	459 (83.5) [4.7]
	$\nu_{14}$	$\delta\text{AsN}_3$ out of phase	<sup>[c]</sup>	257 [2.3]	243 (8.8) [1.4]
	$\nu_{15}$	$\delta\text{As-N-N}$ out of phase	<sup>[c]</sup>	135 [5]	113 (0.4) [5.9]
	$\nu_{16}$	$\tau$ out of phase	<sup>[c]</sup>	<sup>[d]</sup>	44 (0.0) [4.4]

[a] Relative IR and Raman intensities given in parentheses and brackets, respectively.

[b] IR intensities given in  $\text{km mol}^{-1}$  and Raman intensities given in  $\text{\AA}^4 \text{amu}^{-1}$ . [c] Not observed, IR spectrum recorded only between 4000 and 400  $\text{cm}^{-1}$ . [d] Not observed, Raman spectrum recorded only between 4000 and 80  $\text{cm}^{-1}$ . [e] Splittings caused by deviation from  $\text{C}_3$  symmetry, resulting in lifting of the degeneracy. [f] These modes show the following Fermi resonance splittings: IR: 1337 (m) ( $\nu_3 + \nu_{11}$ ) (E); 1133 (mw) ( $\nu_5 + \nu_{11}$ ) (E); Ra: 1334 [0.2] ( $2\nu_3$  or  $2\nu_{11}$ ) (A)  $\text{cm}^{-1}$ . [g] In addition to the listed bands, a Raman band at 191 [1]  $\text{cm}^{-1}$  was observed which was not assigned. It might represent a nitrogen bridge stretching mode.



Table 6. Comparison of observed and unscaled calculated MP2 vibrational frequencies ( $\text{cm}^{-1}$ ) and intensities for  $\text{Sb}(\text{N}_3)_3$ .

		approx. mode description	observed <sup>[a]</sup>		calculated <sup>[b]</sup>
mode		in point group C <sub>3</sub>	IR	Raman	(IR) [Raman]
A	$\nu_1$	$\nu_{\text{as}}\text{N}_3$ in phase	2121 (s,sh)	2123 [7.4]	2183 (631.9) [8.3]
	$\nu_2$	$\nu_s\text{N}_3$ in phase	1243 (vs) <sup>[d]</sup>	1263 [2.2] <sup>[d]</sup>	1243 (114.7) [37.8]
	$\nu_3$	$\delta\text{N}_3$ in phase, in plane		660 [2.4]	653 (0.0) [20.7]
	$\nu_4$	$\delta\text{N}_3$ in phase, out of plane			585 (0.2) [0.5]
	$\nu_5$	$\nu_s\text{SbN}_3$	<sup>[c]</sup>	386 [7.5]	456 (16.0) [39.9]
	$\nu_6$	$\delta\text{SbN}_3$ in phase	<sup>[c]</sup>	289 [0.1]	258 (35.6) [0.8]
	$\nu_7$	$\delta\text{Sb-N-N}$ in phase	<sup>[c]</sup>	115 [4]	91 (0.2) [1.4]
	$\nu_8$	$\tau$ in-phase	<sup>[c]</sup>	<sup>[f]</sup>	78 (0.1) [7.5]
E	$\nu_9$	$\nu_{\text{as}}\text{N}_3$ out of phase	2085 (vs)	2079 [10.0]	2140 (252.0) [14.5]
	$\nu_{10}$	$\nu_s\text{N}_3$ out of phase	1243 (vs) <sup>[d]</sup>	1248 [1.2] <sup>[d]</sup>	1231 (59.1) [5.7]
	$\nu_{11}$	$\delta\text{N}_3$ out of phase, in plane	659 (s)		643 (7.0) [1.9]
	$\nu_{12}$	$\delta\text{N}_3$ out of phase, out of plane	583 (m)		567 (3.3) [0.5]
	$\nu_{13}$	$\nu_{\text{as}}\text{SbN}_3$	<sup>[c]</sup>	370 [3]	414 (70.7) [5.4]
	$\nu_{14}$	$\delta\text{SbN}_3$ out of phase	<sup>[c]</sup>	264 [1.8] <sup>[e]</sup>	199 (9.0) [1.1]
				247 [1.5]	
	$\nu_{15}$	$\delta\text{Sb-N-N}$ out of phase	<sup>[c]</sup>	153 [4] <sup>[e]</sup>	109 (0.2) [7.0]
			141[6.0]		
	$\nu_{16}$	$\tau$ out of phase	<sup>[c]</sup>	<sup>[f]</sup>	56 (0.1) [4.2]

[a] Relative IR and Raman intensities given in parentheses and brackets, respectively. [b] IR intensities given in  $\text{km mol}^{-1}$  and Raman intensities given in  $\text{\AA}^4 \text{amu}^{-1}$ . [c] Not observed, IR spectrum was recorded only between 4000 and 400  $\text{cm}^{-1}$ . [d] These modes show the following Fermi resonance splittings: IR, 1326 (m), ( $\nu_3 + \nu_{11}$ ) (E); 1162 (mw), ( $\nu_5 + \nu_{11}$ ) (E); Ra: 1331 [1.2], ( $2\nu_3$  or  $2\nu_{11}$ ) (A),  $\text{cm}^{-1}$ . [e] Splitting due to lifting of the degeneracy. In the low frequency region, the following additional bands were observed and tentatively assigned: IR: 442 mw,  $\nu\text{SbN}_3$ ; RA: 211 [0.9], corresponding to the 191 [1] band in  $\text{As}(\text{N}_3)_3$ . These Raman bands might represent stretching modes of the nitrogen bridges. [f] Not observed, Raman spectrum recorded only between 4000 and 80  $\text{cm}^{-1}$ .

Figure 1. An ORTEP plot of  $\text{As}(\text{N}_3)_3$  with displacement ellipsoids at the 40% probability level.

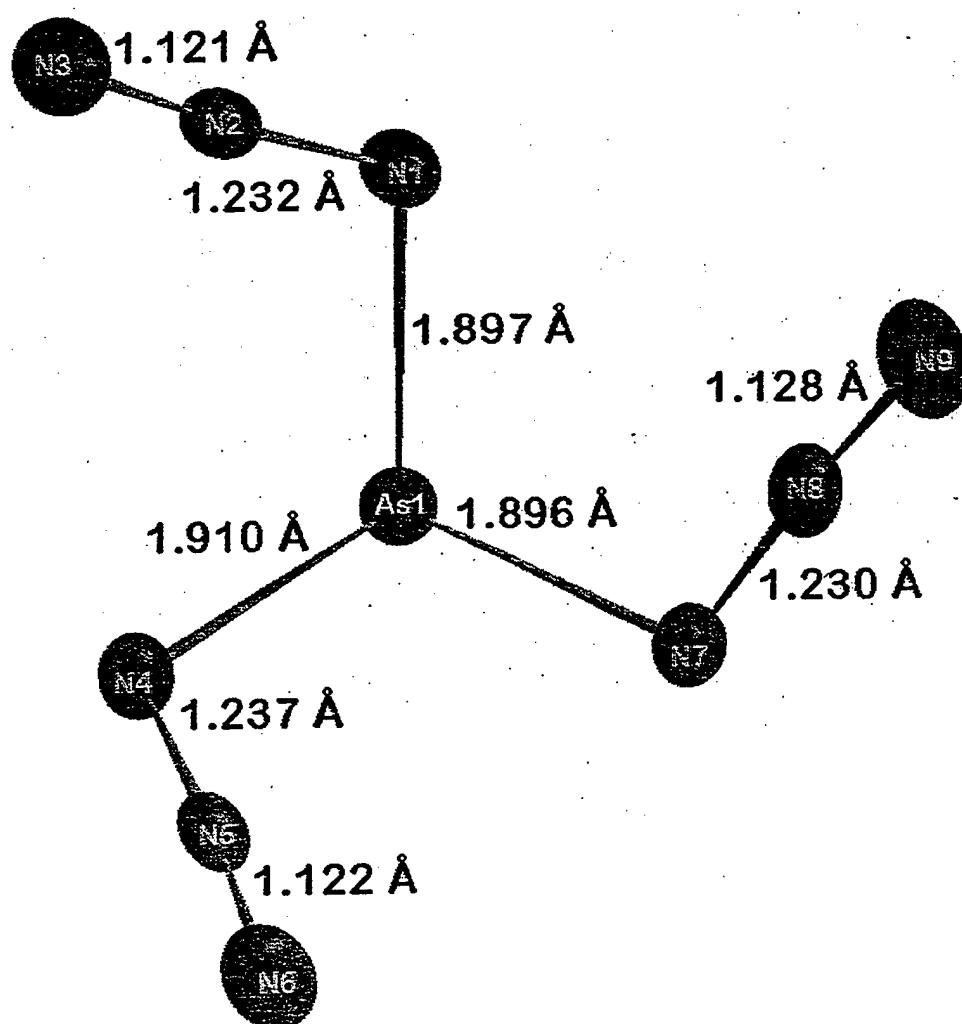


Figure 2. An ORTEP plot of  $\text{As}(\text{N}_3)_3$  at the 40% probability level showing the sterically active free valence electron pair of arsenic and the three closest nitrogen contacts that give the arsenic atom a coordination number of 7.

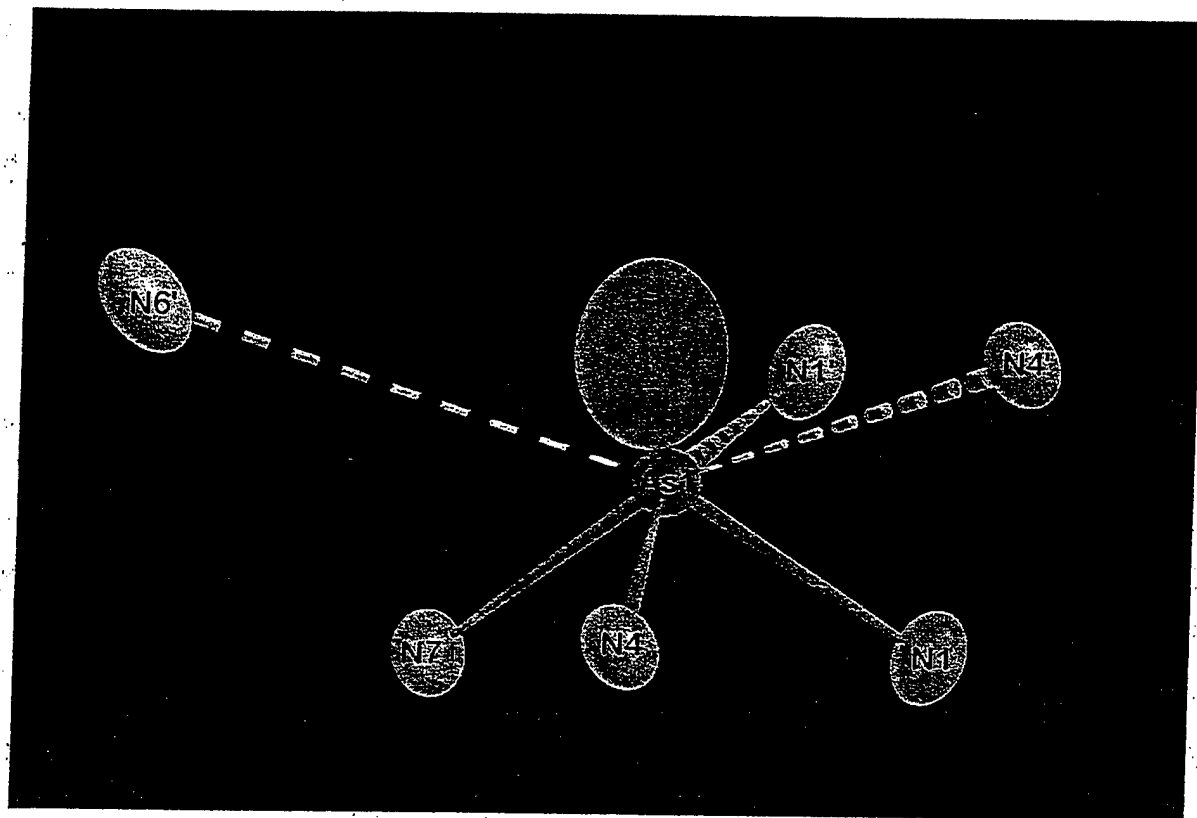


Figure 3. Crystal packing of  $\text{As}(\text{N}_3)_3$  along the  $b$ -axis showing the zig-zag arrangement of alternating  $\text{As}_2\text{N}_4$  and  $\text{As}_2\text{N}_6$  parallelograms. These chains run along the  $a$ -axis and are linked to adjacent chains by  $\text{As1}\dots\text{N6}$  bonds. The  $\text{N7-N8-N9}$  azido groups do not participate in the bridging.

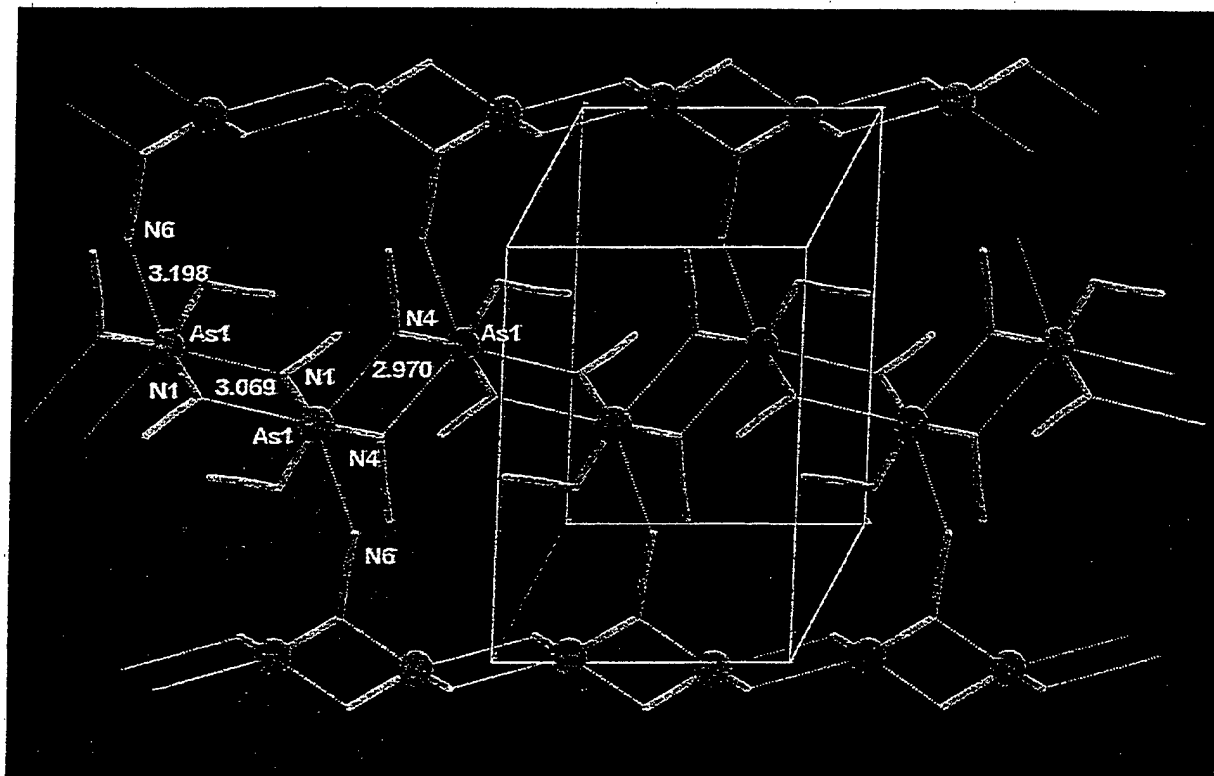


Figure 4: Crystal packing of  $\text{As}(\text{N}_3)_3$ , viewed along the chains and the  $a$ -axis, showing the stacking of the arsenic-nitrogen parallelograms around the inversion centers along the origin and cell edges. The individual chains are linked to each other *via* diagonal As1...N6 contacts which penetrate the  $ab$  plane.

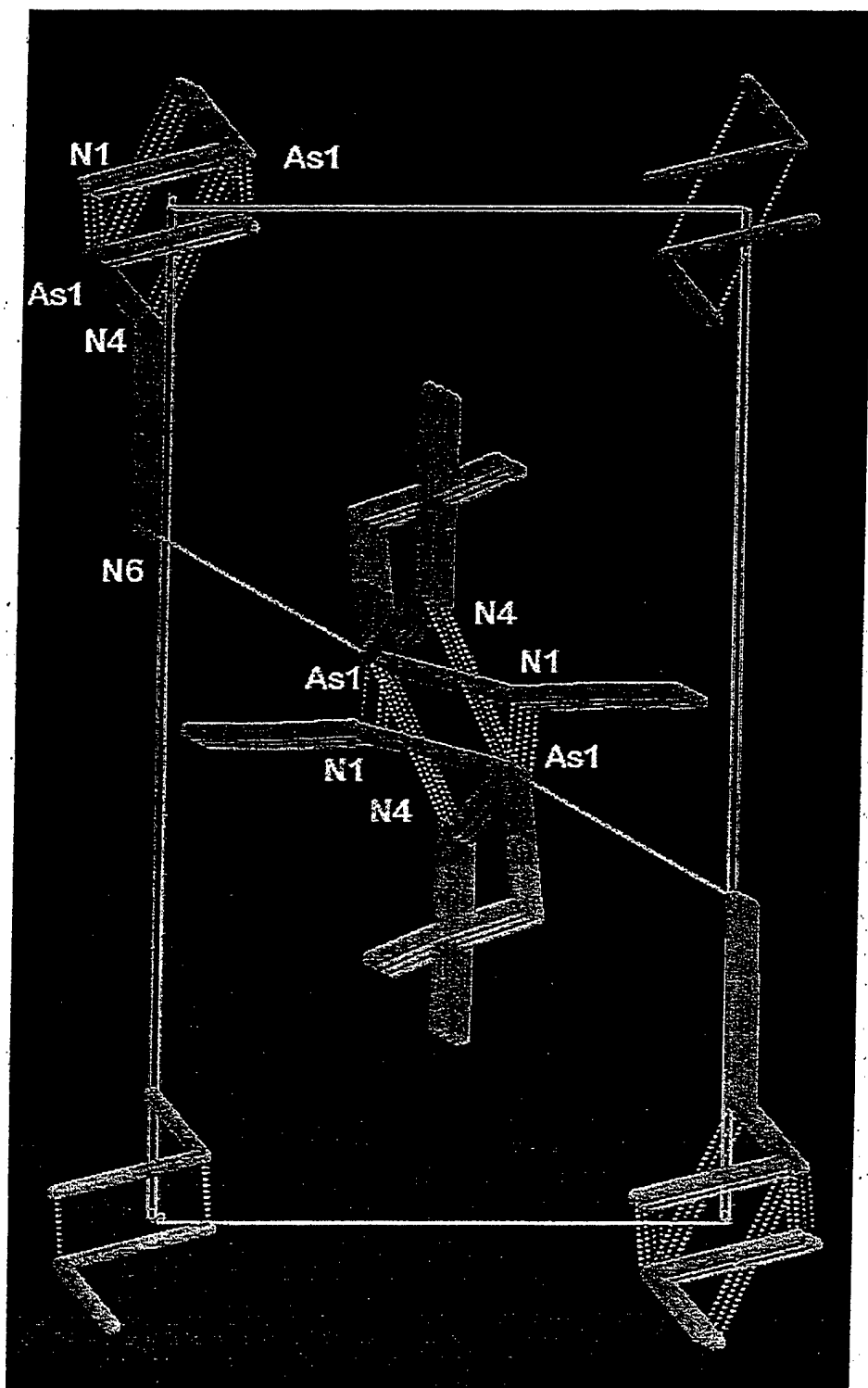


Figure 5. An ORTEP plot of  $\text{Sb}(\text{N}_3)_3$  with displacement ellipsoids at the 40% probability level.

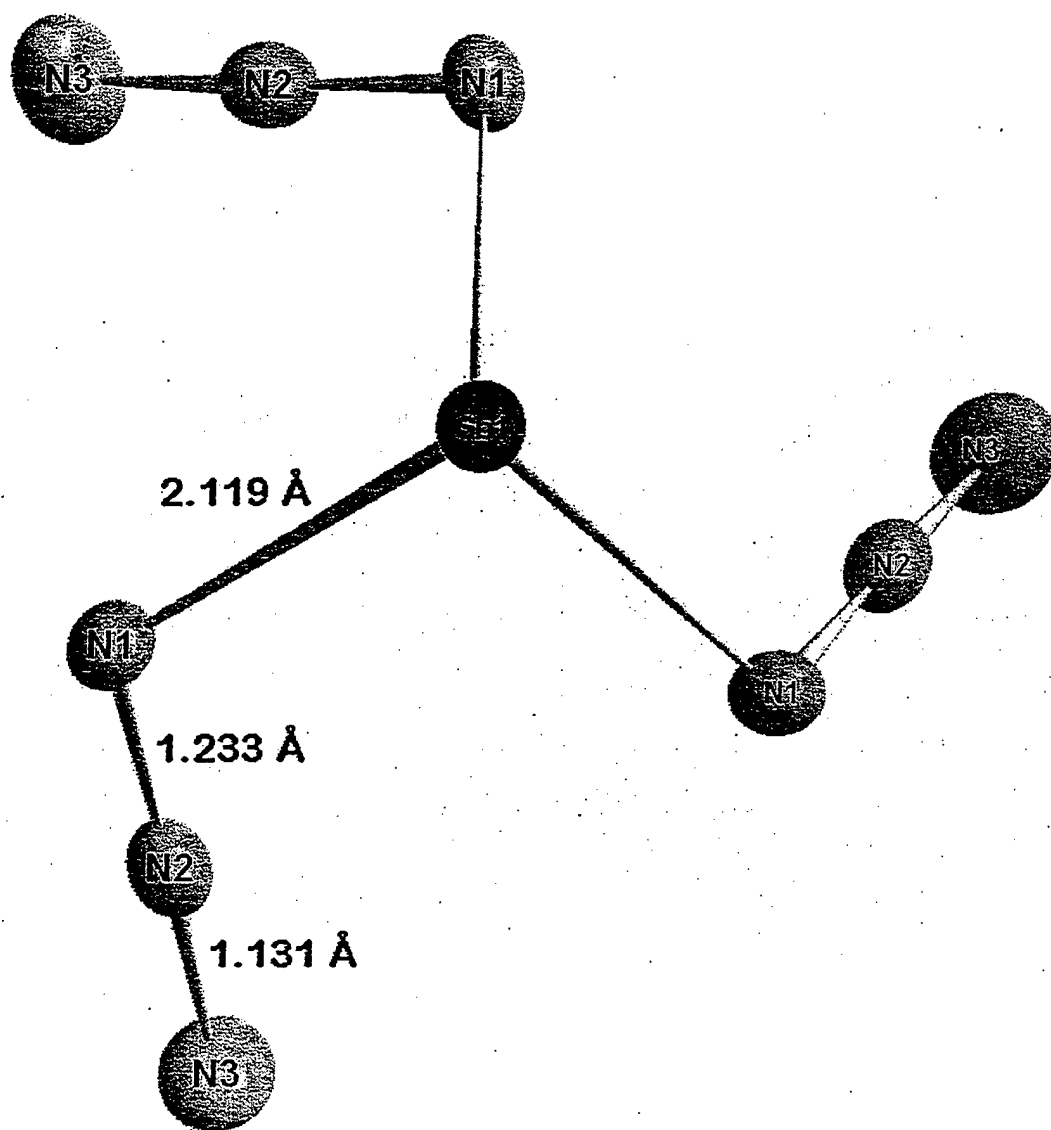


Figure 6. Packing diagrams of  $\text{Sb}(\text{N}_3)_3$  viewed again along the  $z$ -axis. The left picture, in which the nitrogen atoms are highlighted in yellow forms a "Star of David" pattern, while in the right picture, the addition of the connecting bonds emphasizes the six-fold high symmetry of the structure and gives the appearance of a crown made up from "Isle of Man" emblem subunits.

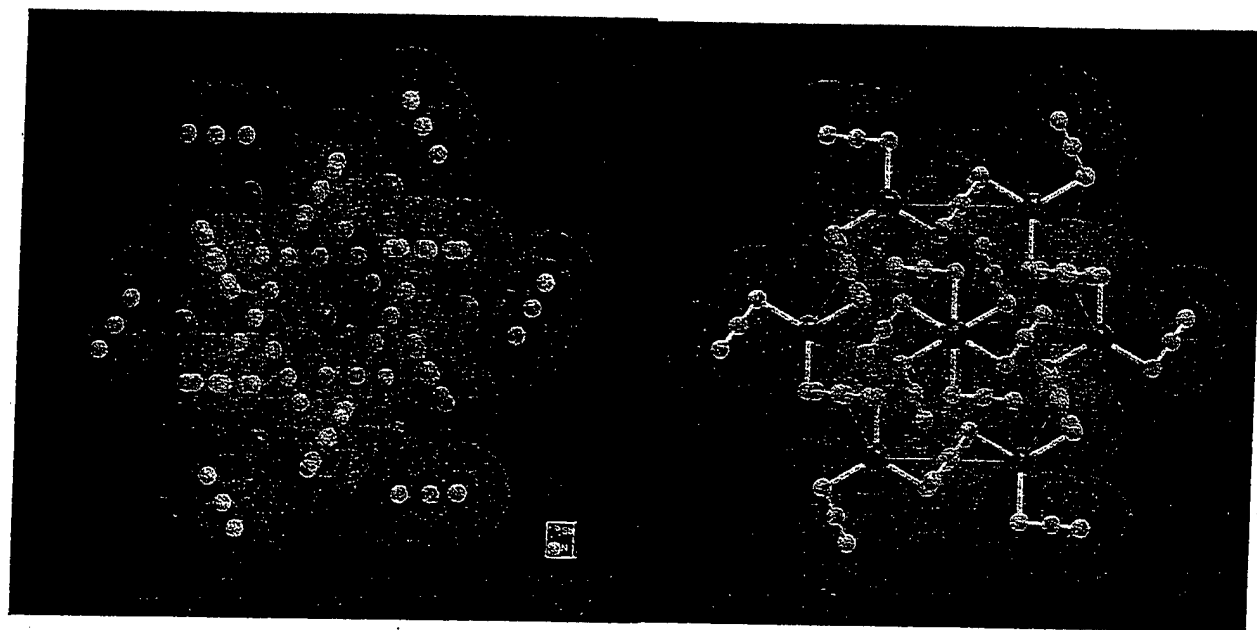


Figure 7. Side view of the  $\text{Sb}(\text{N}_3)_3$  structure showing two sheets interconnected through staggered azido groups.

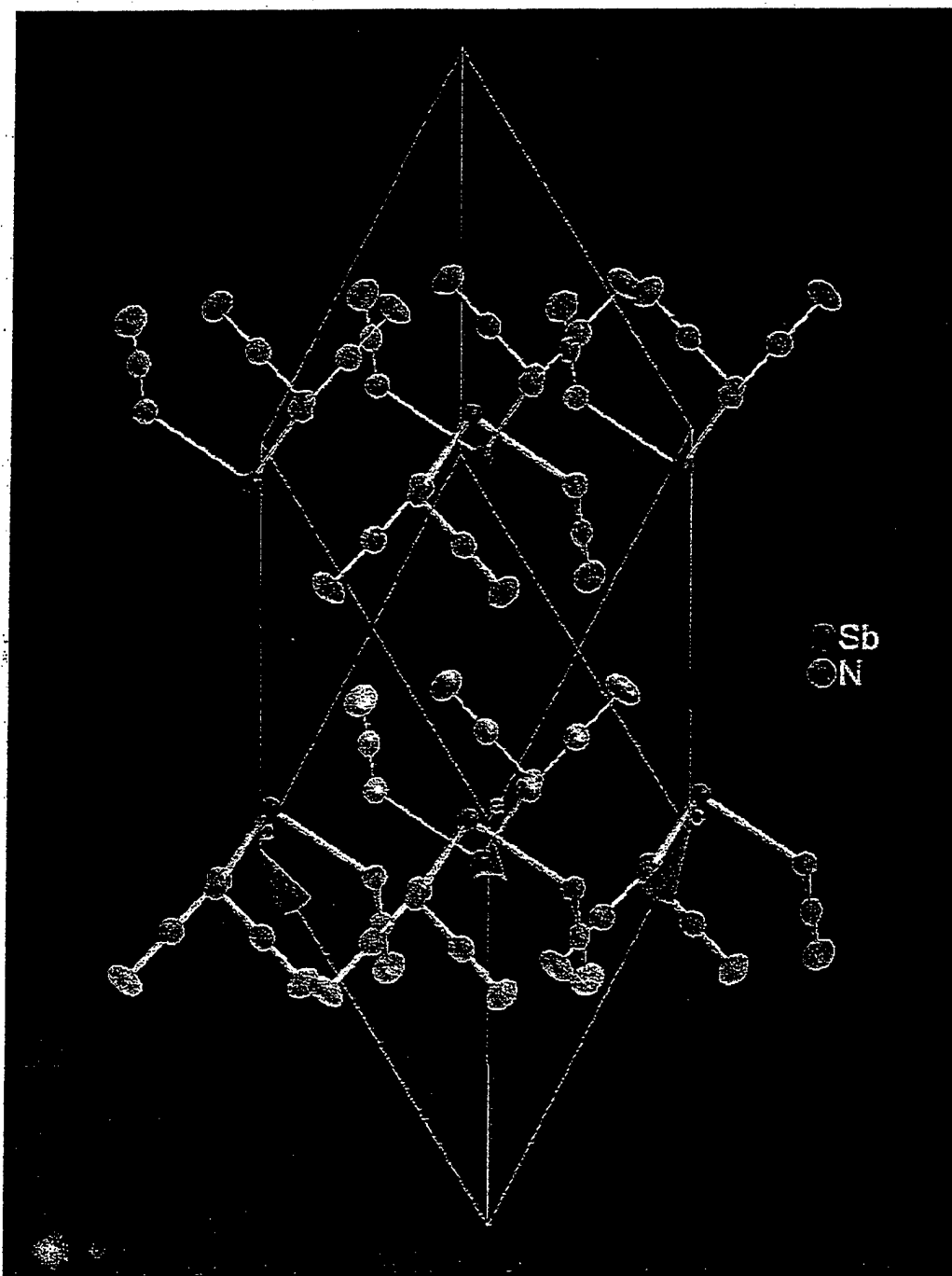




Figure 8. Nitrogen bridging within the  $\text{Sb}(\text{N}_3)_3$  sheets. The insert shows the "Mitsubishi emblem" pattern of the bridging.

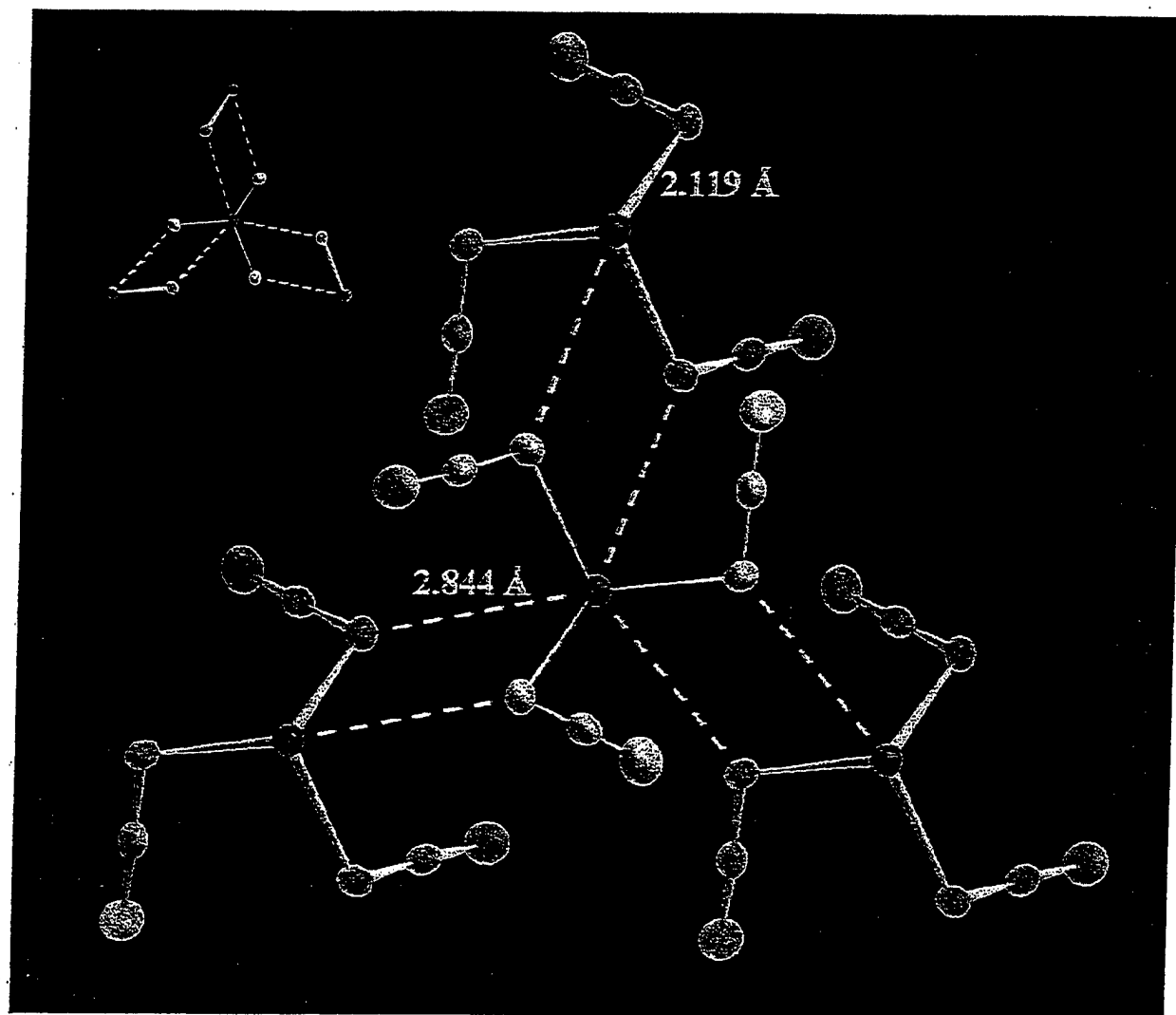


Figure 9. Nitrogen bridging within the  $\text{As}(\text{N}_3)_3$  chains, showing a "Half-Mitsubishi" pattern.

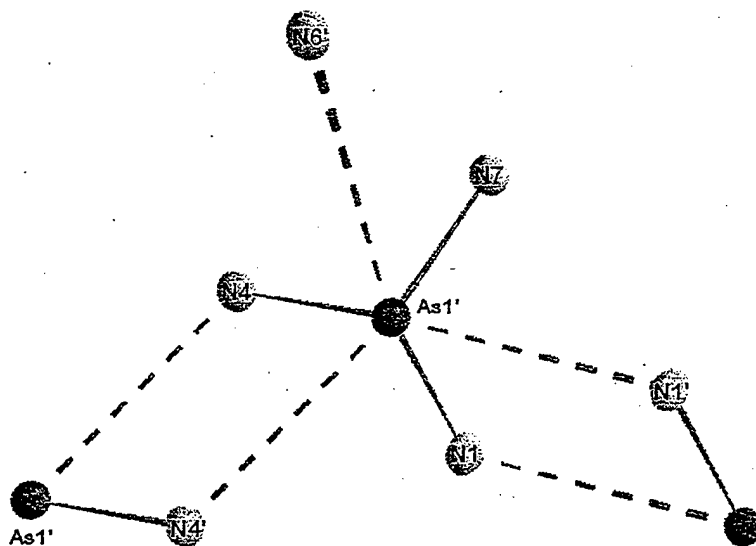
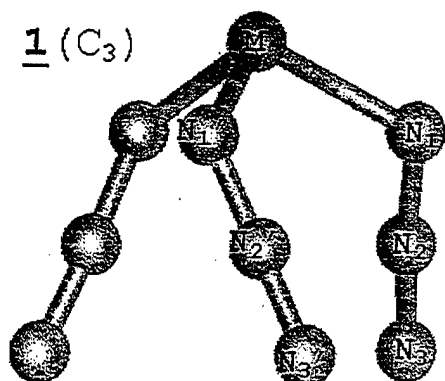
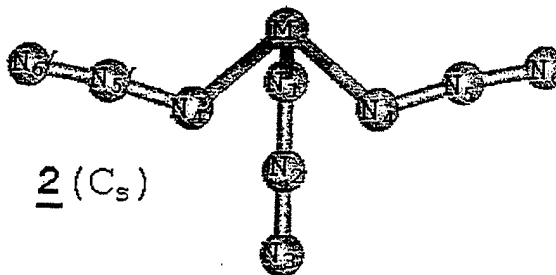


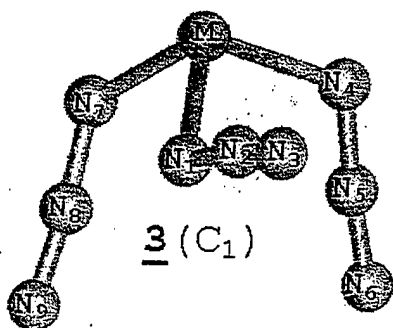
Figure 10. Local minima calculated for  $\text{As}(\text{N}_3)_3$  and  $\text{Sb}(\text{N}_3)_3$  (values given in parantheses) at the MP2 level of theory.



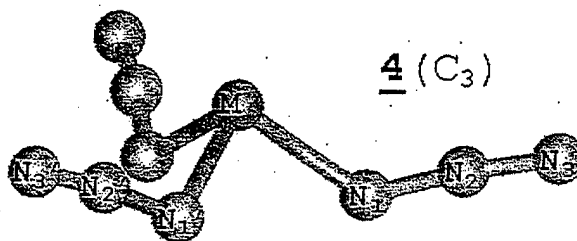
$E = +0.4 \text{ kcal/mol}(0.0)$   
 $R(\text{M}-\text{N}_1) = 1.888(2.069)$   
 $R(\text{N}_1-\text{N}_2) = 1.245(1.267)$   
 $R(\text{N}_2-\text{N}_3) = 1.171(1.196)$   
 $\alpha(\text{N}_1-\text{M}-\text{N}_1') = 99.4(96.2)$   
 $\alpha(\text{N}_2-\text{N}_1-\text{M}) = 117.6(115.1)$   
 $\alpha(\text{N}_3-\text{N}_2-\text{N}_1) = 175.0(174.5)$   
 $\omega(\text{N}_3-\text{N}_2-\text{N}_1-\text{M}) = 164.9(160.6)$   
 $\omega(\text{N}_2-\text{N}_1-\text{M}-\text{N}_1') = 81.7(19.5)$



$E = +0.7 \text{ kcal/mol}$   
 $R(\text{M}-\text{N}_1) = 1.876$   $R(\text{M}-\text{N}_4) = 1.877$   
 $R(\text{N}_1-\text{N}_2) = 1.246$   $R(\text{N}_4-\text{N}_5) = 1.246$   
 $R(\text{N}_2-\text{N}_3) = 1.170$   $R(\text{N}_5-\text{N}_6) = 1.171$   
 $\alpha(\text{N}_1-\text{M}-\text{N}_4) = 99.9$   
 $\alpha(\text{N}_4-\text{M}-\text{N}_1') = 87.1$   
 $\alpha(\text{N}_2-\text{N}_1-\text{M}) = 117.2$   
 $\alpha(\text{N}_5-\text{N}_4-\text{M}) = 117.9$   
 $\alpha(\text{N}_3-\text{N}_2-\text{N}_1) = 174.6$   
 $\alpha(\text{N}_6-\text{N}_5-\text{N}_4) = 172.6$   
 $\omega(\text{N}_3-\text{N}_2-\text{N}_1-\text{M}) = 180.0$   
 $\omega(\text{N}_6-\text{N}_5-\text{N}_4-\text{M}) = 180.0$   
 $\omega(\text{N}_2-\text{N}_1-\text{M}-\text{N}_1') = 44.4$   
 $\omega(\text{N}_5-\text{N}_4-\text{M}-\text{N}_4') = 89.8$   
 $\omega(\text{N}_5-\text{N}_4-\text{M}-\text{N}_1') = 170.7$



$E = 0.0 \text{ kcal/mol}(0.6)$   
 $R(\text{M}-\text{N}_1) = 1.893(2.065)$   $\alpha(\text{N}_1-\text{M}-\text{N}_4) = 98.7(95.3)$   
 $R(\text{M}-\text{N}_4) = 1.883(2.063)$   $\alpha(\text{N}_4-\text{M}-\text{N}_7) = 101.9(98.2)$   
 $R(\text{M}-\text{N}_7) = 1.865(2.046)$   $\alpha(\text{N}_1-\text{M}-\text{N}_7) = 92.5(89.2)$   
 $R(\text{N}_1-\text{N}_2) = 1.243(1.262)$   $\alpha(\text{N}_2-\text{N}_1-\text{M}) = 118.7(120.5)$   
 $R(\text{N}_4-\text{N}_5) = 1.245(1.267)$   $\alpha(\text{N}_5-\text{N}_4-\text{M}) = 118.0(114.5)$   
 $R(\text{N}_7-\text{N}_8) = 1.246(1.268)$   $\alpha(\text{N}_6-\text{N}_7-\text{M}) = 118.8(117.2)$   
 $R(\text{N}_2-\text{N}_3) = 1.172(1.199)$   $\alpha(\text{N}_3-\text{N}_2-\text{N}_1) = 173.6(174.2)$   
 $R(\text{N}_5-\text{N}_6) = 1.171(1.197)$   $\alpha(\text{N}_6-\text{N}_5-\text{N}_4) = 174.7(174.7)$   
 $R(\text{N}_8-\text{N}_9) = 1.169(1.194)$   $\alpha(\text{N}_9-\text{N}_8-\text{N}_7) = 173.6(173.2)$



$E = +3.0 \text{ kcal/mol}$   
 $R(\text{M}-\text{N}_1) = 1.871$   
 $R(\text{N}_1-\text{N}_2) = 1.245$   
 $R(\text{N}_2-\text{N}_3) = 1.171$   
 $\alpha(\text{N}_1-\text{M}-\text{N}_1') = 93.4$   
 $\alpha(\text{N}_2-\text{N}_1-\text{M}) = 118.0$   
 $\alpha(\text{N}_3-\text{N}_2-\text{N}_1) = 172.8$   
 $\omega(\text{N}_3-\text{N}_2-\text{N}_1-\text{M}) = 178.2$   
 $\omega(\text{N}_2-\text{N}_1-\text{M}-\text{N}_1') = 102.3$

Figure 11. Infrared (upper trace) and Raman (lower trace) spectrum of solid  $\text{As}(\text{N}_3)_3$ .

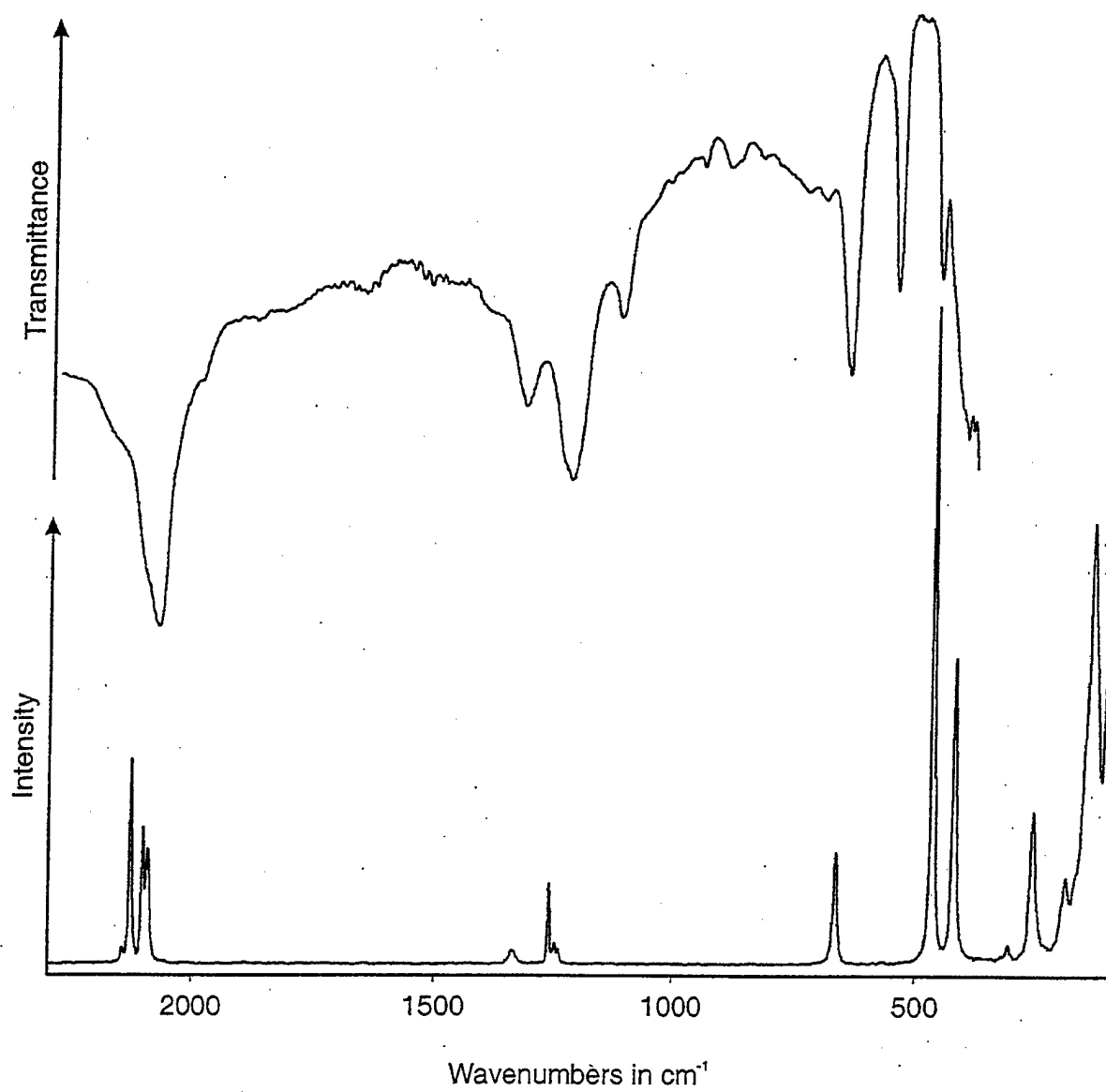
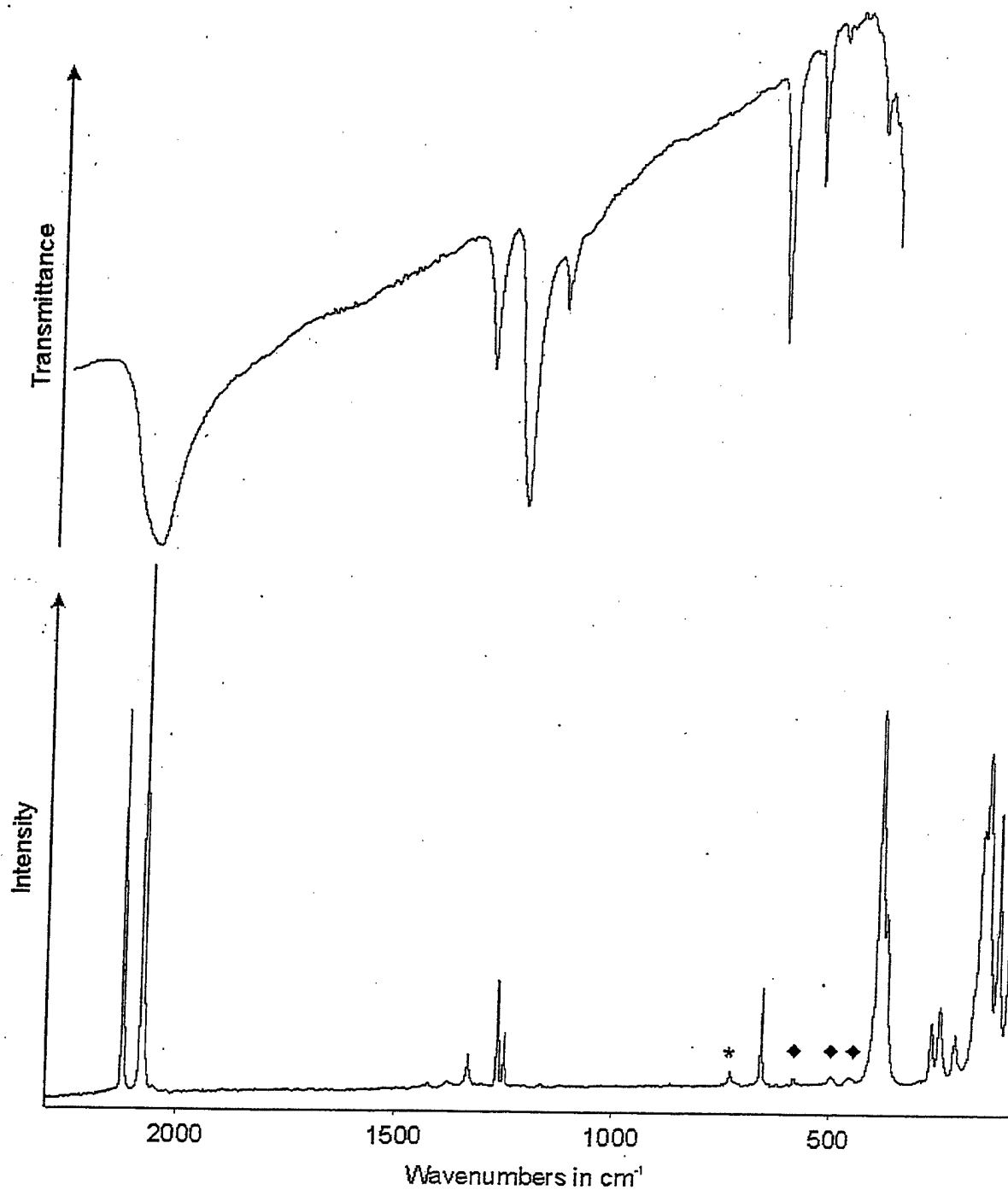


Figure 12. Infrared (upper trace) and Raman (lower trace) spectrum of solid  $\text{Sb}(\text{N}_3)_3$ . The band marked by an asterisk is due to the FEP sample tube. Bands marked by  $\blacklozenge$  are believed to be caused by a small amount of an unknown impurity.



## Synopsis

The structure of  $\text{Sb}(\text{N}_3)_3$  is a fascinating example of perfect rhombohedral  $C_3$  symmetry and exhibits numerous intriguing patterns, while in the closely related  $\text{As}(\text{N}_3)_3$  molecule, subtle crystal packing effects lower the high symmetry.

R. Haiges, A. Vij, J. A. Boatz,  
K. O. Christe\*.....

First Structural Character-  
ization of Binary As(III) and  
Sb(III) Azides

